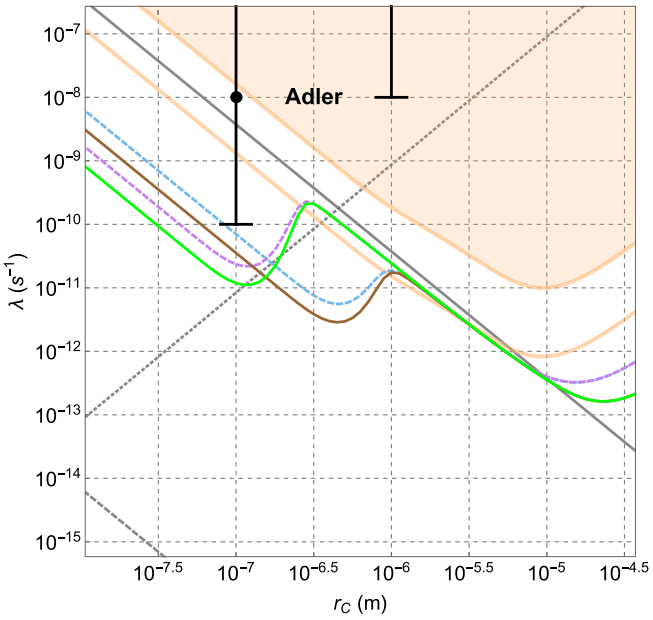

FIG. 6. Hypothetical upper bounds from the multilayer method with a bigger test mass. The system considered here is a cuboid of base side $L = 60\ \mu$m. Dashed purple and blue lines correspond to $M_1 = 1.16 \times 10^{-9}$ kg with $N_{\rm lay} = 48$ and $N_{\rm lay} = 12$, respectively. Green and brown lines correspond to $M_2 = 2.32 \times 10^{-9}$ kg with $N_{\rm lay} = 98$ and $N_{\rm lay} = 25$, respectively. The other lines and the colored region refer to ranges of parameters of CSL, which are already excluded by other experimental data, as described in Fig. 5.

identifying the value for $r_{\rm C}$, if the presence of excess noise were confirmed, by changing the geometry of the resonator. Finally, we emphasize that the hereby proposed scheme to enhance the CSL action can be easily implemented also in other types of mechanical resonators, for example, the one considered in [16,30–32,36–38].

ACKNOWLEDGMENTS

The authors acknowledge support from the H2020 FET project TEQ (Grant No. 766900). A.B. acknowledges financial support from the University of Trieste (through FRA 2016); INFN; the COST Action QTSpace (CA15220); hospitality from the IAS Princeton, where part of this work was carried out; and partial financial support from FQXi.

APPENDIX A: THE CSL ACTION ON LEVITATED SYSTEMS

We compare the CSL contribution $\mathcal{S}_{\rm CSL} = \hbar^2\eta$ to the density noise spectrum $\mathcal{S}_z(\omega)$ for three different cases: a sphere of radius R, a cuboid of lengths (L, L, H), and a cylinder of radius L and height H (moving along the symmetry axis), all made of SiO_2 with density $\mu = 2650$ kg/m^3. The corresponding CSL contributions can be computed analytically [31],

$$\begin{aligned}
\eta_{\rm (sphere)} &= \frac{3\lambda m^2 r_{\rm C}^2}{m_0^2 R^6}\left[R^2 - 2r_{\rm C}^2 + e^{-R^2/r_{\rm C}^2}\left(R^2 + 2r_{\rm C}^2\right)\right],\\
\eta_{\rm (cuboid)} &= \frac{32\lambda m^2 r_{\rm C}^4}{L^4 H^2 m_0^2}\left(1 - e^{-H^2/4r_{\rm C}^2}\right)\\
&\quad\times\left[1 - e^{-L^2/4r_{\rm C}^2} - \frac{L\sqrt{\pi}}{2r_C}\,\mathrm{erf}\left(\frac{L}{2r_{\rm C}}\right)\right]^2,\\
\eta_{\rm (cylinder)} &= \frac{16 m^2 r_{\rm C}^2 \lambda}{H^2 m_0^2 L^2}\left(1 - e^{-H^2/4r_{\rm C}^2}\right)\\
&\quad\times\left\{1 - e^{-L^2/2r_{\rm C}^2}\left[I_0\left(\frac{L^2}{2r_{\rm C}^2}\right) + I_1\left(\frac{L^2}{2r_{\rm C}^2}\right)\right]\right\},
\end{aligned} \tag{A1}$$

where $I_i(x)$ denotes the modified Bessel function.

In Fig. 7 we compare these contributions. As one can see, for small values of the mass, corresponding to a system whose spatial dimension is smaller than $r_{\rm C}$, the CSL diffusion rate depends on the shape in a negligible way. Conversely, for larger masses, or equivalently when the dimensions of the system exceed $r_{\rm C}$, the shape of the system plays a role. The most favorable case is given by the cuboidal geometry, as it can be concluded from Fig. 8, where the cuboidal geometry is compared to the cylindrical one for different values of L (this means that the heights of the two systems will be different). For $L \ll r_{\rm C}$, there

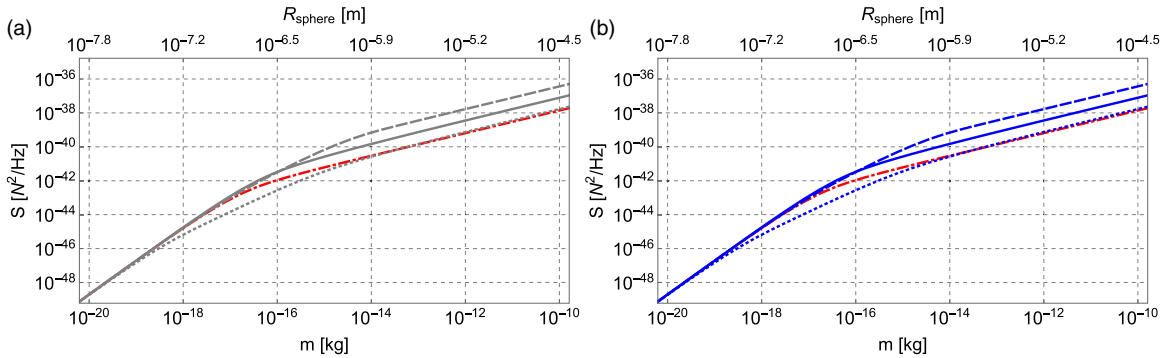

FIG. 7. The CSL contribution $\mathcal{S}_{\rm CSL} = \hbar^2\eta$ to the DNS as a function of the mass of the system; the density has been set equal to $\mu = 2650$ kg/m^3. (For a better comparison, the top axis shows the value of the radius of a sphere with given mass.) (a) Spherical (red dot-dashed line) vs cuboidal (gray lines) geometry. (b) Spherical (red dot-dashed line) vs cylindrical (blue lines) geometry. We considered three different aspect ratios for the cuboidal and for the cylindrical geometries: $L/H = 0.1$ (dotted lines), $L/H = 1$ (solid lines), and $L/H = 10$ (dashed lines). For the CSL parameters, we take as reference Adler's values $\lambda = 10^{-8}\,\mathrm{s}^{-1}$ and $r_{\rm C} = 10^{-7}\,\mathrm{m}$.

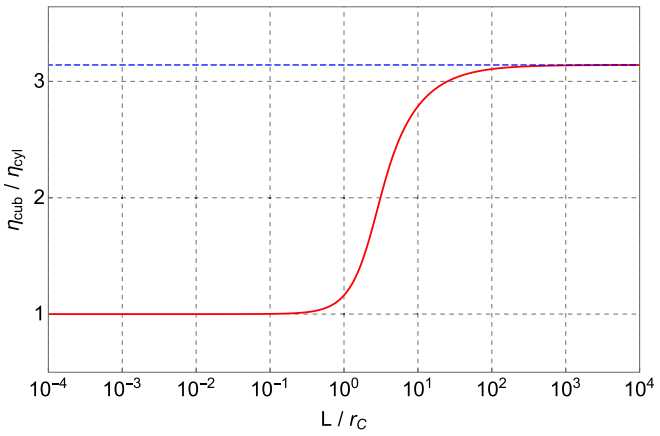

FIG. 8. Comparison of the CSL diffusion rate for a cylinder η_{cylinder} and for a cuboid η_{cuboid}, whose ratio depends only on L/r_C, independently of the mass and density of the system. The blue dashed line corresponds to the asymptotic value π.

is no significant difference between the two geometries, as there is for the sphere. For $L \gg r_C$, the cuboidal geometry has a larger diffusion constant η, which leads to a stronger bound on λ. One can also consider an alternative analysis where the cuboidal and cylindrical geometries are compared for different values of H. In such a case no appreciable differences emerge between the two geometries.

APPENDIX B: MULTILAYER TECHNIQUE

To better understand the enhancement that can be achieved with the multilayer technique, for the sake of simplicity let us compare the single-layer case ($N_{\text{lay}} = 0$) with the two-layer case ($N_{\text{lay}} = 1$) with $\mu_B = 0$. The situation is represented in Fig. 1. The Fourier transform of the mass densities can be derived from Eq. (13), where in the single mass case one has $H = a_1$ and $b_1 = 0$, while in the two-mass case $H = (2a_2 + b_2)$, with $a_1 = 2a_2$, and $b_2 \neq 0$. Thus, one obtains

$$\tilde{\mu}_z^{(N_{\text{lay}}=0)}(k_z) = \frac{2\mu_A}{k_z}\sin(k_z a_2),$$
$$\tilde{\mu}_z^{(N_{\text{lay}}=1)}(k_z) = \frac{4\mu_A \sin\left(\frac{1}{2}k_z a_2\right)}{k_z}\cos\left[\tfrac{1}{2}k_z(a_2+b_2)\right], \quad \text{(B1)}$$

where, to make the comparison more direct, we express both expressions in terms of a_2 and b_2. Due to the different geometry, in the second expression a cosine appears and, by suitably choosing the values of b_2, this gives an enhancement of the CSL effect. In the limit of $r_C \to +\infty$, due to the presence of the Gaussian factor in Eq. (16), only small values of k_z contribute to $\mathcal{I}_z$. This is the case where the collapse noise sees the system as pointlike, regardless of its geometry. In such a limit, the expressions in Eq. (B1) take the same value, $\lim_{k_z\to 0}\tilde{\mu}_z^{(N_{\text{lay}}=0,1)}(k_z) = 2\mu_A a_2$, and thus the corresponding bounds are the same. Conversely, for $r_C \to 0$, one needs to go back to the integrals in Eq. (16), which in our case can be computed exactly and read

$$\mathcal{I}_z^{(N_{\text{lay}}=0)} = \frac{2\sqrt{\pi}\mu_A^2}{r_C}(1 - e^{-a_2^2/r_C^2}),$$
$$\mathcal{I}_z^{(N_{\text{lay}}=1)} = \frac{4\sqrt{\pi}\mu_A^2}{r_C}\left(1 - e^{-a_2^2/4r_C^2} + \tfrac{1}{2}f_{\text{geom}}\right), \quad \text{(B2)}$$

where the first expression is in agreement with Eq. (17) with $H = 2a_2$ and where we defined

$$f_{\text{geom}} = 2e^{-(a_2+b_2)^2/4r_C^2} - e^{-b_2^2/4r_C^2} - e^{-(2a_2+b_2)^2/4r_C^2}, \quad \text{(B3)}$$

which is a geometrical factor explicitly depending on b_2. For $b_2 \neq 0$, in the limit $r_C \to 0$, one finds that the effect in the two-layer case is twice that in the single-layer case: $\lim_{r_C\to 0}\mathcal{I}_z^{(N_{\text{lay}}=1)} = 2\lim_{r_C\to 0}\mathcal{I}_z^{(N_{\text{lay}}=0)} = 4\sqrt{\pi}\mu_A^2/r_C$. This enhancement is due to a geometrical factor, which is different in the two configurations. Something similar happens when the cuboidal and the cylindrical geometries are compared for small values of r_C, as shown in Appendix A. For $b_2 = 0$, one finds that $\lim_{r_C\to 0} f_{\text{geom}} = -1$ and the single-layer result is recovered as expected. One should note, however, that in the limit $r_C \to 0$ one goes beyond the limits of validity of the approximations used in the text.

[1] U. Sinha, C. Couteau, T. Jennewein, R. Laflamme, and G. Weihs, Science **329**, 418 (2010).
[2] B. Hensen *et al.*, Nature (London) **526**, 682 (2015).
[3] L. M. Procopio, L. A. Rozema, Z. J. Wong, D. R. Hamel, K. O'Brien, X. Zhang, B. Dakić, and P. Walther, Nat. Commun. **8**, 15044 (2017).
[4] T. Kovachy, J. M. Hogan, A. Sugarbaker, S. M. Dickerson, C. A. Donnelly, C. Overstreet, and M. A. Kasevich, Phys. Rev. Lett. **114**, 143004 (2015).
[5] O. Usenko, A. Vinante, G. Wijts, and T. H. Oosterkamp, Appl. Phys. Lett. **98**, 133105 (2011).
[6] A. Vinante *et al.* (AURIGA Collaboration), Class. Quantum Grav. **23**, S103 (2006).
[7] B. P. Abbott *et al.* (LIGO Scientific Collaboration and Virgo Collaboration), Phys. Rev. Lett. **116**, 131103 (2016).
[8] B. P. Abbott *et al.* (LIGO Scientific Collaboration and Virgo Collaboration), Phys. Rev. Lett. **116**, 061102 (2016).
[9] M. Armano *et al.*, Phys. Rev. Lett. **116**, 231101 (2016).
[10] M. Armano *et al.*, Phys. Rev. Lett. **120**, 061101 (2018).
[11] C. E. Aalseth *et al.* (The IGEX Collaboration), Phys. Rev. C **59**, 2108 (1999).
[12] S. L. Adler and A. Vinante, Phys. Rev. A **97**, 052119 (2018).
[13] M. Bahrami, Phys. Rev. A **97**, 052118 (2018).
[14] A. Vinante, M. Bahrami, A. Bassi, O. Usenko, G. Wijts, and T. H. Oosterkamp, Phys. Rev. Lett. **116**, 090402 (2016).
[15] A. Vinante, R. Mezzena, P. Falferi, M. Carlesso, and A. Bassi, Phys. Rev. Lett. **119**, 110401 (2017).
[16] M. Carlesso, A. Bassi, P. Falferi, and A. Vinante, Phys. Rev. D **94**, 124036 (2016).

[17] B. Helou, B. J. J. Slagmolen, D. E. McClelland, and Y. Chen, Phys. Rev. D **95**, 084054 (2017).

[18] K. Piscicchia, A. Bassi, C. Curceanu, R. Del Grande, S. Donadi, B. C. Hiesmayr, and A. Pichler, Entropy **19**, 319 (2017).

[19] A. Bassi and G. C. Ghirardi, Phys. Rep. **379**, 257 (2003).

[20] A. Bassi, K. Lochan, S. Satin, T. P. Singh, and H. Ulbricht, Rev. Mod. Phys. **85**, 471 (2013).

[21] G. C. Ghirardi, A. Rimini, and T. Weber, Phys. Rev. D **34**, 470 (1986).

[22] S. L. Adler, J. Phys. A: Math. Theor. **40**, 2935 (2007).

[23] S. L. Adler, J. Phys. A: Math. Theor. **40**, 13501 (2007).

[24] S. Eibenberger, S. Gerlich, M. Arndt, M. Mayor, and J. Tüxen, Phys. Chem. Chem. Phys. **15**, 14696 (2013).

[25] K. Hornberger, J. E. Sipe, and M. Arndt, Phys. Rev. A **70**, 053608 (2004).

[26] M. Toroš, G. Gasbarri, and A. Bassi, Phys. Lett. A **381**, 3921 (2017).

[27] M. Toroš and A. Bassi, J. Phys. A: Math. Theor. **51**, 115302 (2018).

[28] K. C. Lee *et al.*, Science **334**, 1253 (2011).

[29] S. Belli, R. Bonsignori, G. D'Auria, L. Fant, M. Martini, S. Peirone, S. Donadi, and A. Bassi, Phys. Rev. A **94**, 012108 (2016).

[30] M. Bahrami, M. Paternostro, A. Bassi, and H. Ulbricht, Phys. Rev. Lett. **112**, 210404 (2014).

[31] S. Nimmrichter, K. Hornberger, and K. Hammerer, Phys. Rev. Lett. **113**, 020405 (2014).

[32] L. Diósi, Phys. Rev. Lett. **114**, 050403 (2015).

[33] M. Bilardello, S. Donadi, A. Vinante, and A. Bassi, Physica A **462**, 764 (2016).

[34] A. Bassi, A. Großardt, and H. Ulbricht, Class. Quantum Grav. **34**, 193002 (2017).

[35] D. Goldwater, M. Paternostro, and P. F. Barker, Phys. Rev. A **94**, 010104 (2016).

[36] S. McMillen, M. Brunelli, M. Carlesso, A. Bassi, H. Ulbricht, M. G. A. Paris, and M. Paternostro, Phys. Rev. A **95**, 012132 (2017).

[37] B. Schrinski, B. A. Stickler, and K. Hornberger, J. Opt. Soc. Am. B **34**, C1 (2017).

[38] M. Carlesso, M. Paternostro, H. Ulbricht, A. Vinante, and A. Bassi, New J. Phys. (2018), doi:10.1088/1367-2630/aad863.

[39] P. F. Smith and J. D. Lewin, Acta Phys. Polon. **B15**, 1201 (1984).

[40] C. Curceanu, B. C. Hiesmayr, and K. Piscicchia, J. Adv. Phys. **4**, 263 (2015).

[41] F. Laloë, W. J. Mullin, and P. Pearle, Phys. Rev. A **90**, 052119 (2014).

[42] J. Nobakht, M. Carlesso, S. Donadi, M. Paternostro, and A. Bassi, arXiv:1808.01143 (2018).

[43] M. Carlesso, L. Ferialdi, and A. Bassi, arXiv:1805.10100 (2018) [Eur. Phys. J. D (to be published)].

[44] A. Bassi, D.-A. Deckert, and L. Ferialdi, Europhys. Lett. **92**, 50006 (2010).